

## Article

# Increasing the Wear Resistance of Structural Alloy Steel 38CrNi3MoV Subjected to Isothermal Hardening and Deep Cryogenic Treatment

Serhii Bobyr <sup>1,2</sup> , Pavlo Krot <sup>3,\*</sup> , Eduard Parusov <sup>1</sup>, Tetiana Golubenko <sup>1</sup> and Olena Baranovs'ka <sup>1</sup>

<sup>1</sup> Iron and Steel Institute of Z. I. Nekrasov, National Academy of Sciences of Ukraine, 49107 Dnipro, Ukraine; svbobyr07@gmail.com (S.B.); tometal@ukr.net (E.P.); sumer@i.ua (T.G.); elena15dnepr@gmail.com (O.B.)

<sup>2</sup> Department of Material Science and Engineering, KTH Royal Institute of Technology, 10044 Stockholm, Sweden

<sup>3</sup> Faculty of Geoengineering, Mining and Geology, Wrocław University of Science and Technology, 50-370 Wrocław, Poland

\* Correspondence: pavlo.krot@pwr.edu.pl

**Abstract:** In the production of critical parts for various machines and mechanisms, expensive structural steels are used alloyed with chromium, nickel, molybdenum, and vanadium. In practice, the wear resistance of parts, especially under severe operating conditions, may be insufficient due to uneven microstructure and the content of retained austenite. Therefore, increasing the operational stability of various products made of alloy steels is an important task. The purpose of this work is to investigate the effect of isothermal hardening from the intermediate ( $\gamma+\alpha$ )-area and the duration of deep cryogenic treatment on the structure formation and frictional wear resistance of 38CrNi3MoV steel. The isothermal hardening promotes the formation of the required multiphase microstructure of 38CrNi3MoV steel. The influence of the duration of deep cryogenic treatment on the microhardness, amount of retained austenite, fine structure parameters, and friction wear of 38CrNi3MoV steel are established. Complex heat treatment of 38CrNi3MoV steel, according to the proposed mode, makes it possible to achieve a significant decomposition of retained austenite to martensite, which leads to an increase in frictional wear resistance of ~58%.

**Keywords:** alloy steel 38CrNi3MoV; isothermal hardening; deep cryogenic treatment; microhardness; wear resistance



**Citation:** Bobyr, S.; Krot, P.; Parusov, E.; Golubenko, T.; Baranovs'ka, O. Increasing the Wear Resistance of Structural Alloy Steel 38CrNi3MoV Subjected to Isothermal Hardening and Deep Cryogenic Treatment. *Appl. Sci.* **2023**, *13*, 9143. <https://doi.org/10.3390/app13169143>

Academic Editor: Manoj Gupta

Received: 12 July 2023

Revised: 6 August 2023

Accepted: 9 August 2023

Published: 10 August 2023



**Copyright:** © 2023 by the authors. Licensee MDPI, Basel, Switzerland. This article is an open access article distributed under the terms and conditions of the Creative Commons Attribution (CC BY) license (<https://creativecommons.org/licenses/by/4.0/>).

## 1. Introduction

Today, to produce various parts of industrial machines—mill rolls, shafts of power-generating equipment—structural steels are used alloyed with different elements (Cr, Ni, Mo, V), such as 38CrNi3MoV steel, which is investigated in this work. This steel has a high stability of austenite in the range of 400–500 °C [1–5]. Studies on the mechanical properties and microstructure of 38CrNi3MoV steel have been carried out in a significant number of works [1–5]. For steels with high austenite stability, a step-like mode or isothermal cooling is often used [3]. It was proposed that isothermal treatment of 38CrNi3MoV steel from the intermediate ( $\gamma+\alpha$ )-area should be used to increase its wear resistance [5]. The nearest steel analogues, 35NiCrMoV12-5 (DIN) and 4340 (AISI), are used for special-purpose products, and were studied in previous works [6,7].

The reliability of finished products from alloy steels depends significantly on the homogeneous distribution of structural components and the unavoidable content of retained austenite (RA), which can reach 10–15% after quenching. Alloying elements shift the finish temperature ( $M_f$ ) of martensite transformation below zero. Therefore, the high-temperature tempering does not reduce RA to zero. Hence, increasing the operational stability of finished products made of carbon alloy steels while obtaining the most favorable combination

of the mechanical parameters (hardness, wear resistance, and toughness) is an important scientific and technical task.

It is well known that deep cryogenic treatment (DCT) can significantly increase the properties of alloy steels [8–11]; thus, it is used as a final treatment for many technologies and industries, such as materials science [12,13], tool and steel industries [14–18], manufacturing of rolls [19], and automotive industry [20]. This process uses sub-zero temperature, below  $-125\text{ }^{\circ}\text{C}$ , which is created by liquid nitrogen [18], as the preferred cooling medium. Both gaseous and liquid coolants are applied, but steel sample interaction with a liquid coolant creates higher internal stresses. The achieved changes in the steel parts are almost permanent and irreversible under normal thermal conditions. In addition, DCT is a low-cost, environmentally friendly, non-toxic, and safe technology.

The influence of DCT at a temperature of  $-196\text{ }^{\circ}\text{C}$  and subsequent tempering at  $200\text{ }^{\circ}\text{C}$  on the microstructure of tungsten carbide (WC-Co) rock cutting bits is investigated in [21]. Different durations of low-temperature treatment are applied (from 6 to 36 h, with 6 h steps). The authors explained the observed phase shift in a binder (Co) by the differences in the thermal expansion coefficient and thermal shear stress. The optimum duration of DCT based on the wear resistance of samples was determined as 24 h.

The AISI D6 tool steel properties (microstructure, impact toughness, and wear resistance) subjected to DCT is investigated in [22]. Different routes were considered: quenching–tempering, quenching–tempering (single and double)–DCT. The authors concluded that double tempering after DCT produces the best mechanical properties and the same wear resistance due to the precipitation of fine carbides. The soaking time (2 and 24 h) was considered less influential than double tempering on the final properties.

The influence of the DCT effect on microscale abrasion of AISI D2 tool steel is represented in [23]. The best wear resistance was achieved when the DCT was performed immediately after tempering. The authors relate this effect to the transformation of RA in martensite and the formation of fine secondary carbides.

The wear and fatigue properties of H21 tool steel subjected to DCT are investigated in [24]. The DCT step ( $-185\text{ }^{\circ}\text{C}$ ) was applied before and after double tempering ( $540\text{ }^{\circ}\text{C}$ ) with subsequent soft tempering ( $100\text{ }^{\circ}\text{C}$ ). The obtained results show that the wear rate was reduced by 24% and surface roughness by 21%, and the fatigue limit increased by 13%.

Corrosion properties of various high-speed steels subjected to DCT are analyzed in [25]. The results show that microstructure, hardness, and corrosion resistance change to different extents depending on the chemical composition of the samples.

A comprehensive review of DCT application is represented in [26]. Based on numerous studies, it was concluded that shallow cryogenic treatment, only up to  $-80\text{ }^{\circ}\text{C}$ , has less effect than DCT up to  $-196\text{ }^{\circ}\text{C}$ . Under both treatments, some steel grades showed reduced fatigue limit, while for other steels it increased. An optimal soaking time of about 36 h was noted for D2 steel. Precipitation of secondary carbides was considered the main factor of higher wear resistance due to the larger interface created with the matrix. A reduction in the wear rate of about 14% for AISI A8 subjected to DCT before tempering corresponded to a higher number of secondary carbides by 6%, and increased from 0.68% to 0.73% of the covered area [27].

Less represented in the literature, multistage cryogenic treatment (MCT) of X153CrMoV12 cold work steel was tested in [28]. Both MCT and DCT produced similar changes in the microstructure, and increased the amounts of homogeneous refined carbides. The effects of multiple DCT and tempering on microstructure and properties of high carbon bearing steels are shown in [29].

Summarizing the metallurgical principles of microstructure formation in DCT [30], we can conclude that one of its primary objectives is the transformation of RA to martensite. This is one of the theoretically explained mechanisms for wear resistance increasing because the martensitic phase has much higher hardness than the initial austenite phase [31]. Typically, this phase transformation has been investigated and quantified via the X-ray diffraction (XRD) method [32–35]. The authors of this work used such a method, along

with an ultrasonic method and electron microscopy with a microanalyzer, to observe the transformations of RA.

In addition to the RA transformation, another mechanism for wear resistance improvement by DCT is the secondary alloy carbides precipitated and uniformly distributed by the tempering [36–39] or DCT itself [40]. In some studies of tool steels, it is stated that the DCT process promotes the diffusion of carbon atoms to dislocations [41–46], and these cluster atoms contribute to an increase in the number of carbides during tempering. However, other authors believe that carbon atoms do not diffuse at the temperatures of DCT [47,48], and that immobile carbon atoms are captured by gliding dislocations [49].

Another hypothesis for improved wear resistance is a higher dislocation density in the steel structure obtained after DCT. However, despite the repeated mention of this in the literature [48–50], quantitative analysis of the dislocation density is seldom possible. Hence, the question regarding the influence of DCT on the dislocation density of doped alloys remains unanswered; we set out to investigate it using the XRD method.

Another important unresolved issue is the influence of a part's holding time in the coolant. It has been reported that DCT of martensitic steels conducted for a longer period has a better effect on the wear resistance [8,40,51]. However, according to a generally assumed theory of martensitic transformation, austenite to martensite transformation has to occur right after a certain level of temperature is reached, and additional time has no effect on martensite fraction volume. In addition, due to low diffusion rate, significant changes are not expected at such low temperatures [48]. On the other hand, most researchers use significant DCT exposure times (24 h or more) to obtain significant changes in the structure and distribution of carbides [8,10,13,18,33,40,51].

The analyzed literature shows that although the general principles of DCT are known, and its effects have been previously investigated on many alloy steels, these results do not guarantee that proposed heat treatment routes will be successfully replicated on any other similar steel grade, e.g., 38CrNi3MoV. Many additional factors (carbon content and deviation of chemical composition, temperature of austenitization, quenching and tempering routes) play an important role in the final efficiency of DCT. Therefore, the practical implementation of known principles requires additional research for every steel grade.

The originality of our idea lies in the development of a complex mode of stepwise isothermal hardening from the intermediate ( $\gamma+\alpha$ )-area, combined with DCT. This made it possible to improve the uniformity of the distribution of structural components, significantly reduce the amount of retained austenite and, accordingly, increase the resistance to frictional wear of 38CrNi3MoV steel. The developed mode of combined processing is characterized by higher energy efficiency compared to the traditional technology of hardening with high-temperature tempering of structural alloy steels. In addition, the influence of the holding time of DCT on structure formation and wear resistance is experimentally studied, of which the optimal value has been discussed with conflicting options in the literature.

## 2. Materials and Methods

### 2.1. Selected Material

The samples of 38CrNi3MoV alloy steel produced by PJSC «DNIPROSPETSSTAL» (Zaporizhzhya, Ukraine) were taken after soft annealing. The chemical composition of the steel in wt.% is 0.40 C, 0.31 Mn, 0.28 Si, 1.28 Cr, 3.12 Ni, 0.43 Mo, 0.15 V.

### 2.2. Structure Analysis

The standard instrumentation was used for sample treatment for optical and scanning electron microscopy, which was performed using an optical microscope Axiovert 200 MAT (Carl Zeiss, Oberkochen, Germany) and an electron high-resolution microscope/microanalyzer JAMP 9500F (JEOL, Tokio, Japan). The amount of RA was determined by the ultrasonic method on the UT-1 device according to the developed method. X-ray diffraction (XRD) was used to quantify parameters of fine structure and crystalline lattice.

Measurements by XRD were conducted with a diffractometer DRON-3.0 using Cu K $\alpha$  radiation and a Cr filter.

### 2.3. Mechanical Properties Measurement

Hardness and microhardness were measured on TK-2 and PMT-3M instruments, respectively. Hardness and microhardness were calculated as average values based on the results of 5 and 10 measurements, with accuracies of  $\pm 1$  unit and  $\pm 200$  MPa, respectively. The wear resistance of the test samples ( $\varnothing 40.0 \pm 0.1$  mm, thickness 10 mm, weight up to 82 g) was determined using the SMC-2 testing machine at a constant speed of rotation of the driving shaft (300 rpm). The value of slippage of the sample and the counter body was kept kinematically at 10%, and the pressing force was set at 800 N. Wear was determined by the loss of mass of the samples for 60,000 rotations of the sample, with an accuracy of 0.0001 g.

### 2.4. Heat Treatment

The experimental heat treatment technology included heating and holding the steel samples at a temperature of 750 °C for 20 min, cooling to the temperature of isothermal holding (650–400 °C) in air, holding for 20 min in a furnace, and cooling in air. A chamber for DCT, which was used in this research, was designed and manufactured by the Institute of Physics NAS of Ukraine (Kyiv, Ukraine). Cooling in the cryogenic treatment chamber was achieved using liquid nitrogen after its gasification. Its flow was regulated by a digital controller of temperature. Samples were treated at  $-196$  °C with a cooling rate of 1 °C per minute. Holding times were installed as 10 min, 1 h, and 22 h. After DCT, samples were heated to room temperature at a rate of 1 °C per minute. Schemes of the basic mode of heat treatment and including the DCT stage are represented in Figure 1.

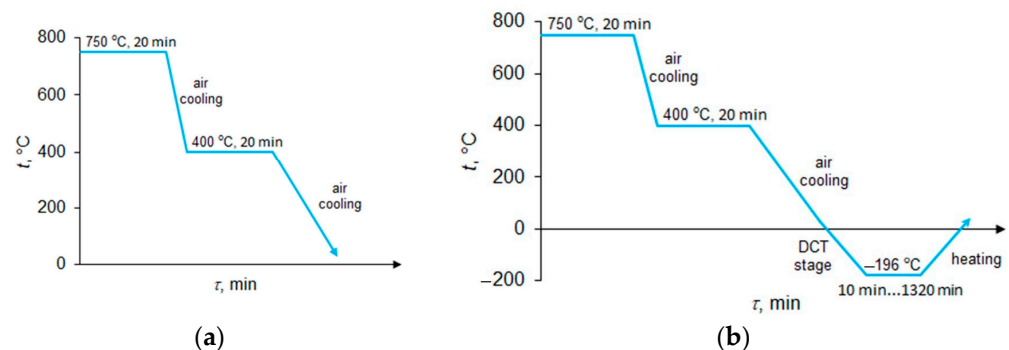


**Figure 1.** Schemes of heat treatment of 38CrNi3MoV steel: (a) basic mode, (b) basic mode + DCT.

## 3. Results

### 3.1. Structure Formation under Isothermal Hardening

To increase the wear resistance of 38CrNi3MoV steel products while ensuring the required hardness (less than 40 HRC before machining), the option of obtaining a multiphase troostite–bainite–martensite structure was considered [3,4]. As a technology that allows one to obtain such a structure, isothermal hardening was used [5].

The hardness of the investigated samples depending on the temperature of isothermal holding is shown in Figure 2, and their microstructures are presented in Figure 3.

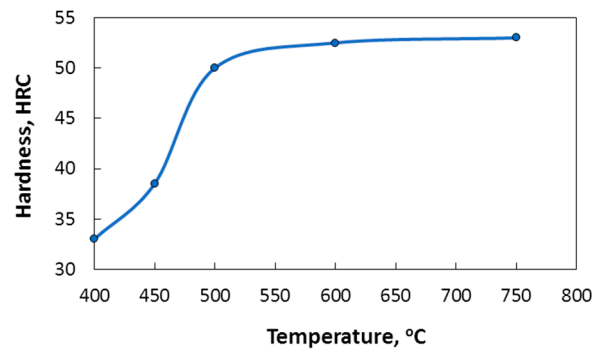


**Figure 2.** Dependence of steel hardness on isothermal holding temperature.

The microstructure of steel at isothermal holding temperatures of 750–600 °C consisted mainly of martensite with high hardness (Figure 3a). At the isothermal holding temperature of 500 °C, a small amount of troostite was formed in the steel structure (see Figure 3b). The amount of troostite increased with the decrease in isothermal holding temperature (Figure 3c,d). When holding 38CrNi3MoV steel at the temperature of 750 °C for 20 min, no primary ferrite was precipitated. Upon subsequent cooling, structural components of the eutectoid and quasi-eutectoid types were formed.

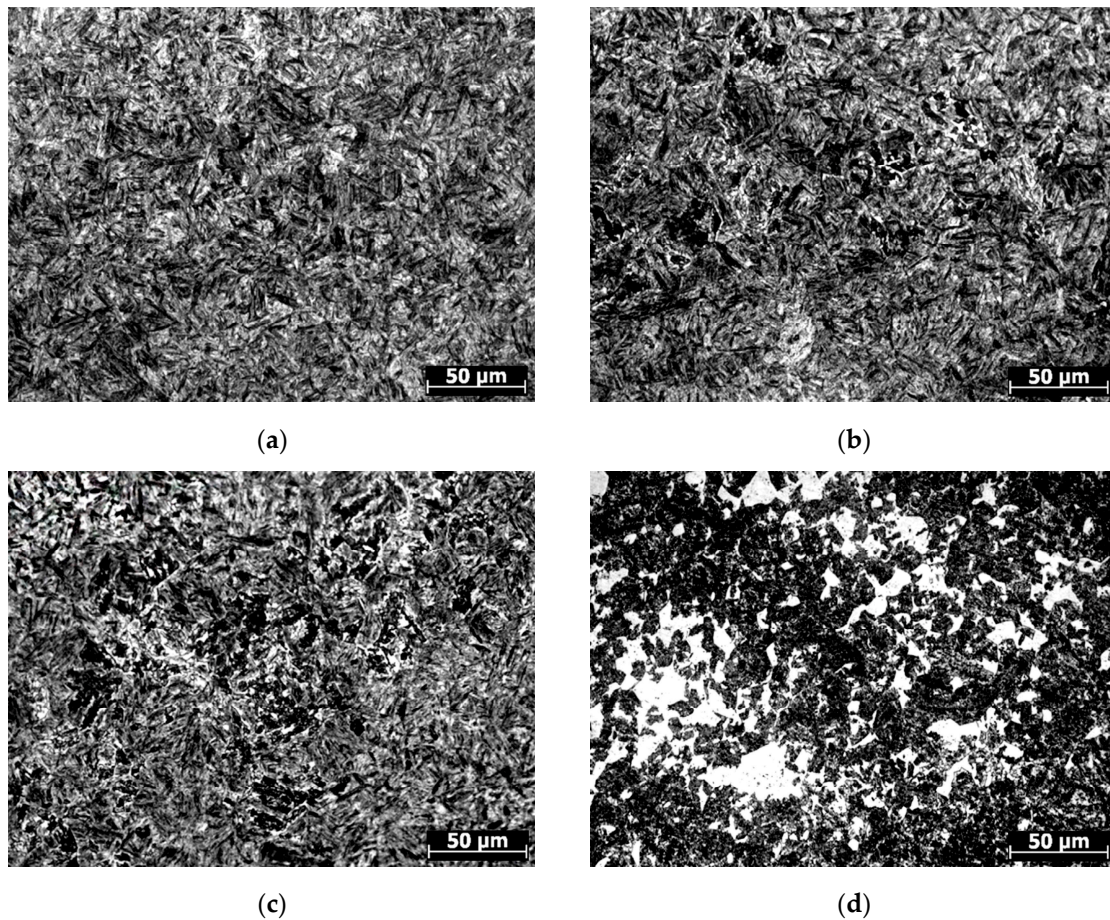


**Figure 3.** Microstructures of 38CrNi3MoV steel samples after isothermal treatment at 600 °C (a), 500 °C (b), 450 °C (c), and 400 °C (d).

Steel hardness had the required values (less than 40 HRC) at the holding temperature of 450–400 °C. The basic mode of heat treatment guaranteed the initial hardness of 38CrNi3MoV steel of less than 40 HRC, and the stabilization of RA (see Figures 3d and 4).

The microstructure of the sample processed by this mode consisted mainly of troostite (homogeneous areas), with a microhardness of 3620 MPa, and light inhomogeneous areas of bainite + RA, with a microhardness of 6350 MPa (Figure 4a,b).

The bainite of steel, which was formed in 38CrNi3MoV steel during the isothermal treatment, contained particles of carbides, predominantly of cementite type, light small particles of 0.2–1.0  $\mu\text{m}$  in size (Figure 4c). The steel structure also had areas with high austenite contents and semi-coherent precipitation of carbide particles (Figure 4d).

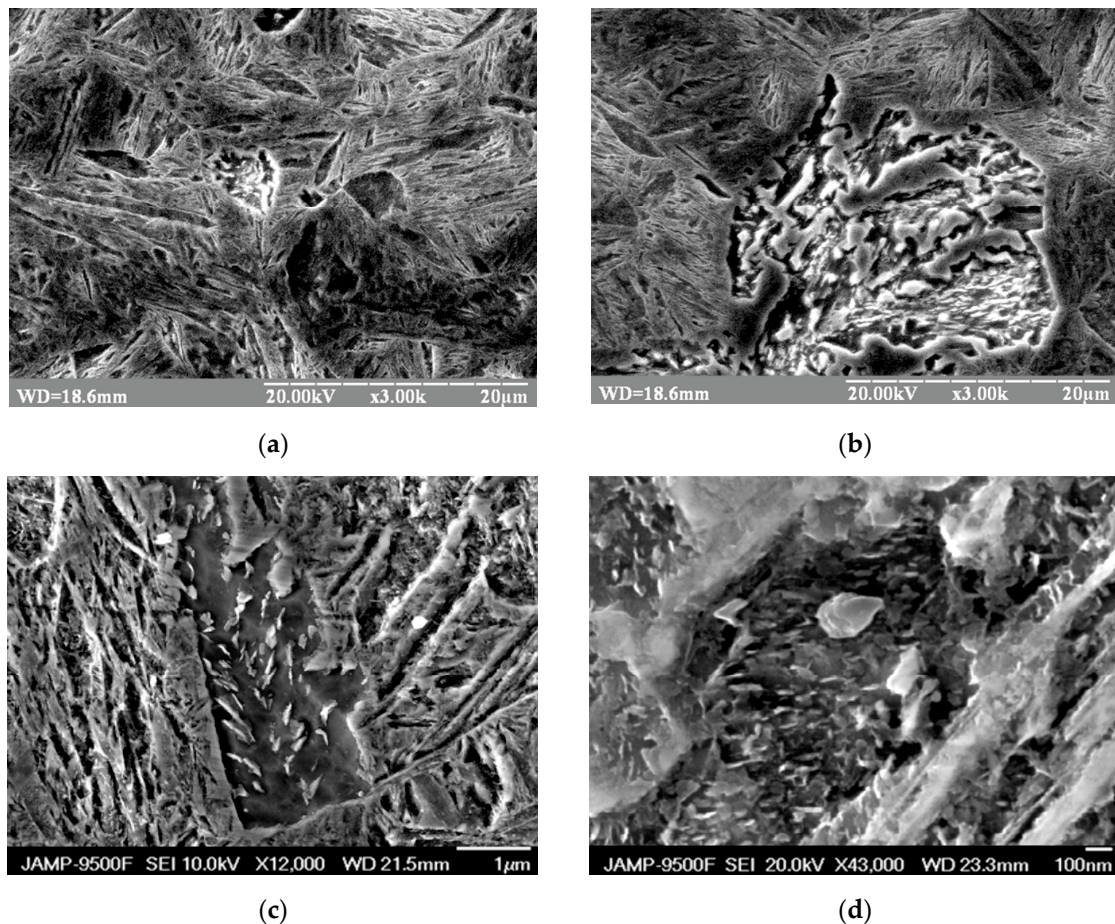


**Figure 4.** Microstructures of 38CrNi3MoV steel samples after isothermal treatment at 750 °C for 20 min, cooling to 400 °C, holding for 20 min, cooling in the air (see description in the text): (a,b) troostite (homogeneous areas) and bainite + RA (inhomogeneous areas); (c,d) the bainite structure of steel with carbides.

The subsequent X-ray microanalysis showed (see Figure 5 and Table 1) that the quasi-eutectoid and bainitic components were formed mainly in the inter-dendritic areas of the structure, with high contents of nickel, silicon, chromium, and molybdenum, while vanadium was uniformly distributed in the solid solution.

Holding the steel at an intermediate temperature of 750 °C contributed to the release of these carbides and the stabilization of RA, which was part of the bainite–austenite formations. The amount of RA reached values of about 10.8%.

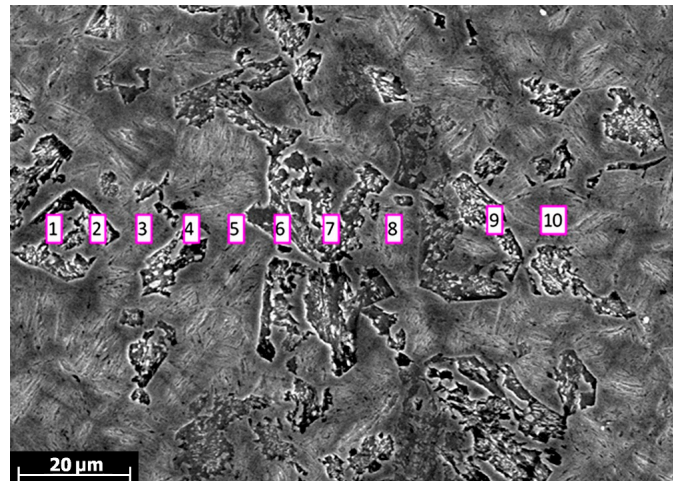


**Figure 5.** X-ray microanalysis of 38CrNi3MoV steel sample after isothermal heat treatment (see Table 1 for values 1–10).

**Table 1.** Values of chemical element contents for the different points in Figure 5.

Points	V	Cr	Mn	Si	Ni	Mo	Fe
1	0.00	1.21	0.48	0.34	2.87	0.17	94.93
2	0.06	1.02	0.21	0.18	3.11	0.69	94.73
3	0.00	0.96	0.53	0.37	3.41	0.22	94.51
4	0.00	1.15	0.39	0.29	3.18	0.49	94.50
5	0.09	0.89	0.44	0.31	2.74	0.51	95.02
6	0.00	1.07	0.26	0.33	2.68	0.37	95.29
7	0.00	1.17	0.18	0.26	3.03	0.32	95.04
8	0.00	0.88	0.59	0.41	2.91	0.46	94.75
9	0.11	0.81	0.48	0.44	2.74	0.53	94.89
10	0.00	1.28	0.55	0.38	3.09	0.44	94.26

### 3.2. Structure Formation under Deep Cryogenic Treatment (DCT)

The following cryogenic treatment had a significant effect on the microhardness of the structural components of steel (Figure 6a) and the amount of RA (Figure 6b). This indicates that the use of DCT in the heat treatment contributed towards the RA transformation into martensite. The increase in microhardness obtained for the 38CrNi3MoV steel samples was about 22.3%. Measurements of the content of RA both by the X-ray and ultrasound methods confirm its metastability and tendency towards transformation during DCT (Figure 6b).

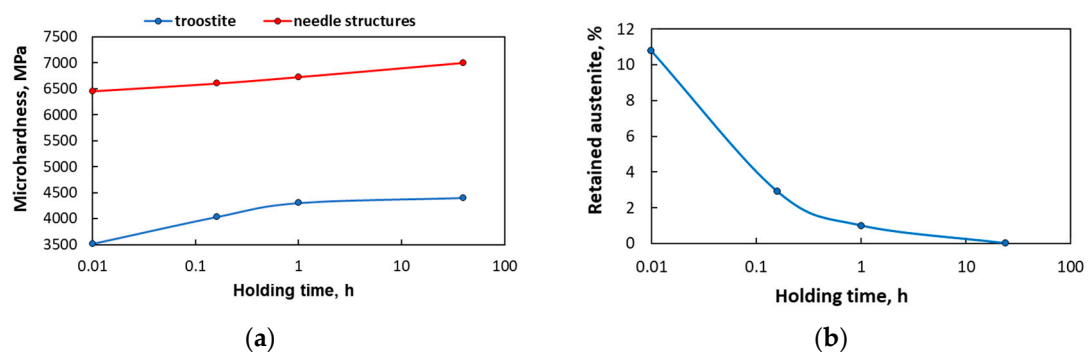


**Figure 6.** Influence of DCT holding time on the microhardness of structural components (a) and the amount of RA (b) in the 38CrNi3MoV steel.

The transformation of RA into martensite during DCT is fully confirmed by the electron microscopic investigation of the steel structure (see Figure 7).

These microstructures clearly show how the RA in the form of globules (Figure 7a,b), needles (Figure 7c) and packets (Figure 7d) transformed into martensite of the corresponding morphology. Figure 7d shows, that one part of the austenite grain has turned into a martensite packet, and the other part has been preserved as RA.

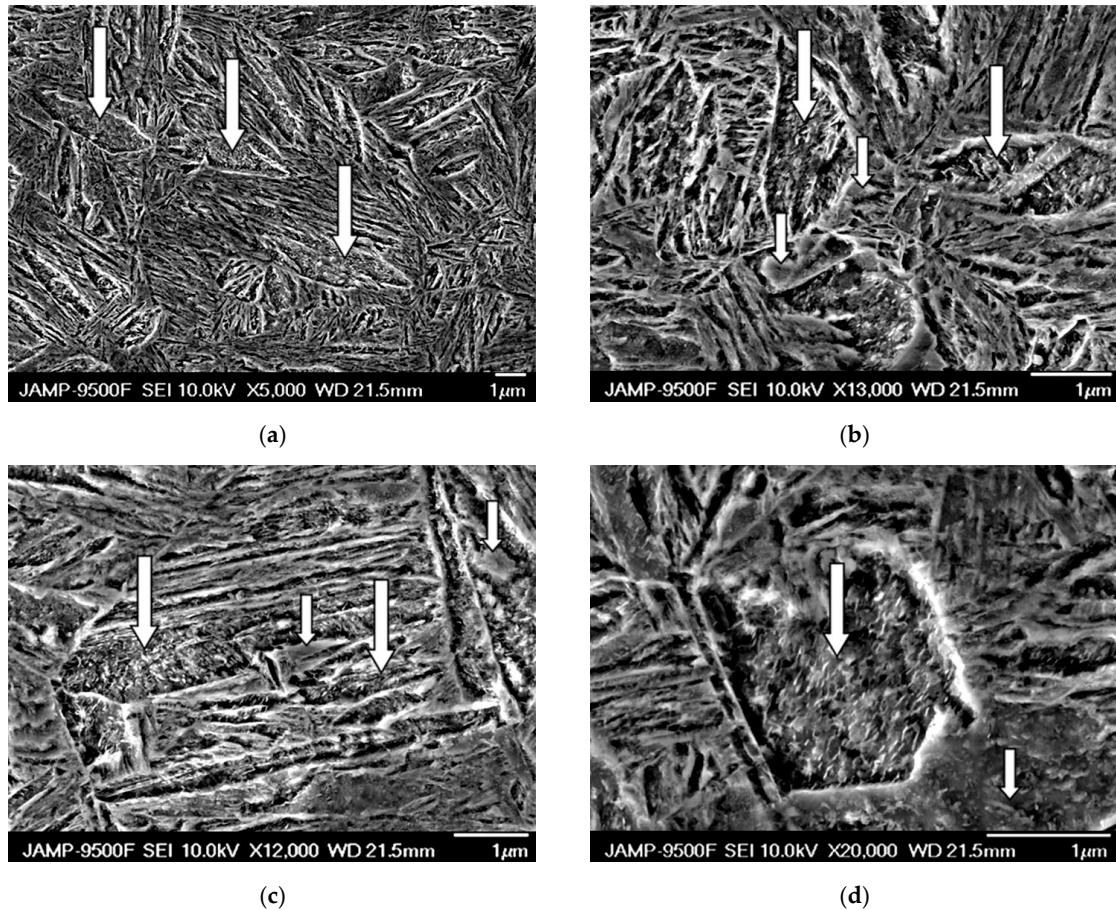


**Figure 7.** Microstructures of 38CrNi3MoV steel after cryogenic treatment for 10 min (large arrows—martensite, small arrows—retained austenite): (a,b) martensite in the form of globules; (c) needles; (d) packets.

Increasing the exposure time of the samples at liquid nitrogen temperature had almost no effect on the microstructure of the samples observed using a light microscope (Figure 8a,b), but affected both the microhardness of the structural components and the content of RA. When held for 10 min in liquid nitrogen, the largest amount of RA was converted and the microhardness of the steel increased significantly (Figure 6a).

Holding samples at the temperature of liquid nitrogen for a longer time contributed to the further transformation of RA, increased microhardness (Figure 6a), and the formation of finer martensitic laths [38,39] (Figure 8c,d). A possible mechanism for such a process will be discussed below.

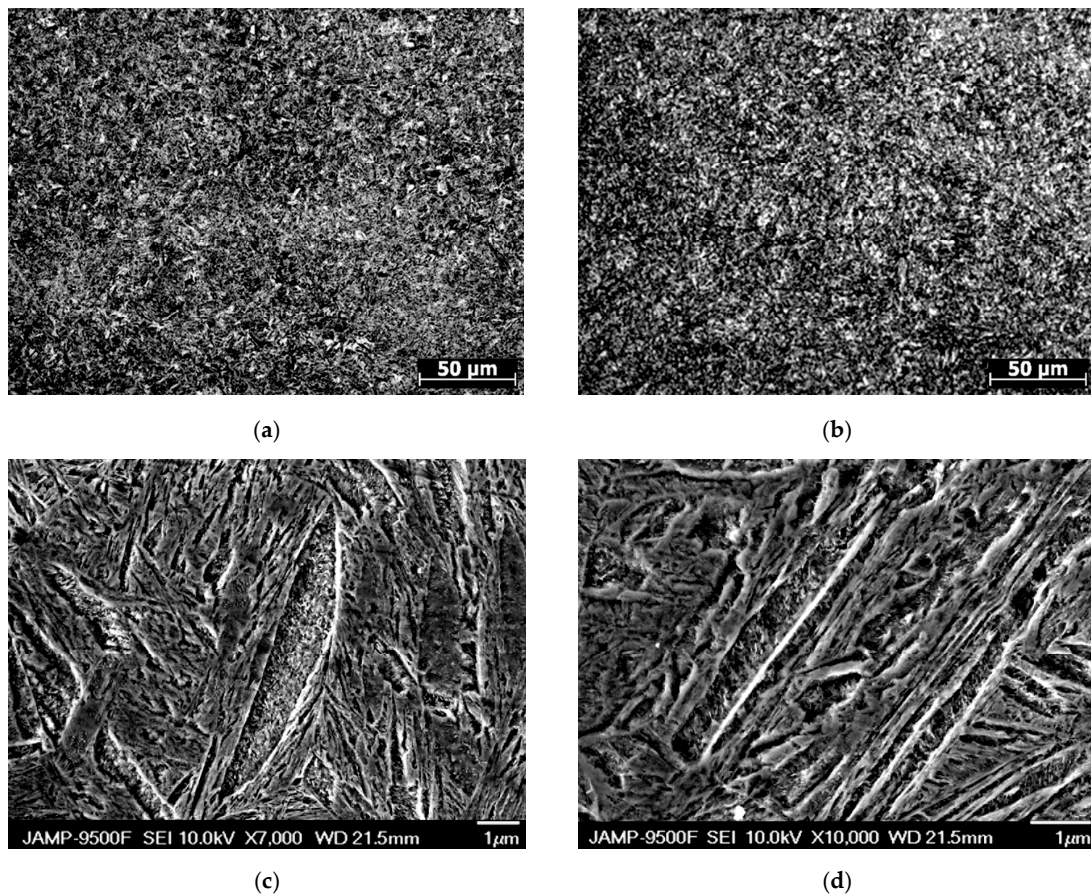


**Figure 8.** Microstructures of 38CrNi3MoV steel samples after cryogenic treatment for 1 h (a,c) and 22 h (b,d).

Cryogenic treatment of steel for 10 min followed by heating had practically no effect on the distribution of alloying elements in the structure (see Figure 9 and Table 2). The exception was vanadium, which became more isolated, presumably in carbide inclusions.

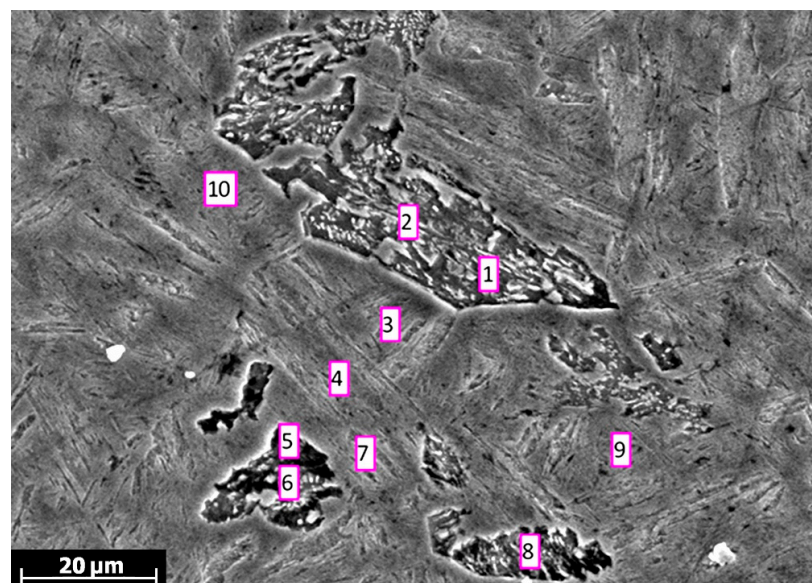


**Figure 9.** X-ray microanalysis of 38CrNi3MoV steel after isothermal heat treatment + DCT 10 min (see Table 2 for values 1–10).

**Table 2.** Values of chemical element contents for the different points in Figure 9.

Points	V	Cr	Mn	Si	Ni	Mo	Fe
1	0.00	1.01	0.47	0.31	3.01	0.34	94.86
2	0.00	1.22	0.49	0.35	3.22	0.52	94.20
3	0.01	0.99	0.19	0.26	2.74	0.37	95.44
4	0.08	0.88	0.21	0.23	3.21	0.46	94.93
5	0.00	0.85	0.41	0.39	2.87	0.41	95.07
6	0.00	0.98	0.44	0.45	2.64	0.54	94.95
7	0.00	0.85	0.58	0.52	2.75	0.61	94.69
8	0.17	0.92	0.61	0.47	3.09	0.18	94.56
9	0.00	0.84	0.66	0.49	2.77	0.62	94.62
10	0.11	1.10	0.28	0.38	3.07	0.39	94.67

#### 4. Discussion

Comparative testing of 38CrNi3MoV steel samples treated under different modes showed high wear resistance of 38CrNi3MoV steel samples after experimental treatment and its increase during cryogenic treatment (Table 3).

The basic mode of hardening (quenching with low tempering) provided a high hardness of 38CrNi3MoV steel with the lowest wear resistance. Thus, the increased hardness of alloyed steel is not a guarantee of its high wear resistance. Isothermal hardening, according to experimental modes from temperatures of 850 °C and 750 °C, resulted in higher wear resistance, by 29% and 48%, respectively, of 38CrNi3MoV steel as compared to the usual hardening mode.

Experimental mode of hardening from the two-phase area and DCT within 1 h provided a significant 58% increase in the wear resistance of 38CrNi3MoV steel. Hence, this mode can be the most efficiently applied for the heat treatment of critical parts of 38CrNi3MoV steel.

**Table 3.** Effect of treatment type on hardness RA content and wear of 38CrNi3MoV steel.

No	Treatment Modes	Hardness, HRC	Retained Austenite, %	Wear, %
1	850 °C, oil quenching, tempering at 230 °C, 2 h	47.5	7.7	0.159
2	850 °C, isothermal hardening at 230 °C, 2 h	46.0	9.5	0.112
3	750 °C, cooling to 400 °C, 20 min, air cooling (basic mode)	36.3	10.8	0.083
4	Basic mode + DCT 10 min	41.5	2.6	0.078
5	Basic mode + DCT 1 h	43.3	1.2	0.066
6	Basic mode + DCT 22 h	45.7	0.3	0.072

In the samples of investigated steel, DCT for 10 min led to the transformation of soft austenite into hard martensite, which resulted in higher hardness (Table 3). In these samples, decreases in block sizes and increases in microdistortions of the crystal lattice in steel were found (Table 4) after DCT. First, this was caused by the volume change of the newly formed martensite, which led to the multiplication of dislocations and an increase in stresses.

**Table 4.** Effect of DCT holding time on the parameters of fine structure and crystal lattice in 38CrNi3MoV steel.

No	Treatment Modes	Parameter $a_{110}$ , Å	Size of Blocks $D$ , nm	Magnitude $\Delta a/a \times 10^{-3}$	Density $\rho \times 10^{12}$ , cm <sup>-2</sup>
1	Basic mode	2.8609	11.3	2.1	3.9
2	Basic mode + DCT 10 min	2.8645	8.6	3.9	6.7
3	Basic mode + DCT 1 h	2.8668	5.2	3.3	8.4
4	Basic mode + DCT 22 h	2.8652	4.1	3.0	10.1

The second possible mechanism may be related to local thermal stresses. The atomic probe tomography of quenched steel performed in [34] showed that there are local clusters enriched in carbon, which agrees with our electron microscopy data. Experimental studies of Fe-C alloys [52,53] have shown the significant dependence of thermal expansion on the carbon concentration and increases in coefficient differences at low temperature. Differences in local thermal expansion cause increased microstress, leading to dislocation multiplication [39,54]. Hence, in our case, it can be assumed that inhomogeneous distribution of carbon and other elements [34,55] creates carbon clusters and nanocarbides in microareas of metastable austenite. They have a thermal expansion coefficient different from the main matrix, which leads to local stresses,  $\gamma \rightarrow \alpha$  lattice transformation, and dislocation multiplication upon cooling to cryogenic temperatures. Clusters of carbon upon subsequent heating to room temperature are sites for the formation of additional dispersed carbides in the structure of alloyed steel [11,12,34,38,55].

Part of the resulting microstresses can be gradually removed during longer cryogenic holding by a local isothermal transformation of metastable austenite into fine acicular martensite [37] with small block sizes (Table 4, Figure 7c,d). An increase in the exposure time at cryogenic temperatures, therefore, can promote a reduction in the parameter  $a$  value and microdistortions in the crystal lattice of steel, and increase its dislocation density as a result of the isothermal formation of martensite [56,57].

The processes occurring during DCT affect the wear resistance of alloy steel. In our case, an increase in holding time at cryogenic temperature to 22 h did not lead to a higher wear resistance, presumably due to its increased hardness and brittleness in the absence of RA. The samples of alloyed steel, hardened according to the generally accepted technology, and having high hardness, also had reduced wear resistance (Table 3).

## 5. Conclusions

1. In order to create a multiphase structure of 38CrNi3MoV steel containing RA (7.5–10.8%), isothermal hardening at the  $(\gamma+\alpha)$ -area is proposed. When holding 38CrNi3MoV steel at the temperature of 750 °C for 20 min, no primary ferrite was formed. Upon subsequent cooling, structural components of the eutectoid and quasi-eutectoid types were formed. A significant effect of isothermal holding temperature on the structure and hardness of alloyed steel has been established. The bainite of steel contained particles of carbides, predominantly of cementite type, 0.2–1.0 microns in size, which were formed during the isothermal treatment of 38CrNi3MoV steel.
2. Using X-ray microanalysis, it was shown that quasi-eutectoid and bainitic components were formed mainly in the inter-dendritic sections of the steel structure, with high contents of nickel, chromium, and molybdenum.
3. The use of DCT, according to the proposed mode of hardening of 38CrNi3MoV steel, resulted in a significant transformation of RA into martensite, increasing microhardness by 22.3%.
4. Isothermal hardening of 38CrNi3MoV steel at the  $(\gamma+\alpha)$ -area contributed to an increase in wear resistance compared to traditional heat treatment modes.
5. Application of DCT to 38CrNi3MoV steel for 10 min led to the transformation of austenite into martensite, increasing hardness and wear resistance. In the experimental samples of 38CrNi3MoV steel, the block sizes decreased and microdistortions of the crystal lattice increased.
6. The experimental mode of hardening and DCT with a holding time of 1 h provided the greatest increase (by 58%) in the hardness and wear resistance of 38CrNi3MoV steel, and can be recommended for implementing as a hardening technology for critical metal parts.
7. An increase in the DCT time to 22 h did not lead to an increase in the wear resistance of 38CrNi3MoV steel, presumably due to an increase in hardness and brittleness in the absence of RA. Samples of 38CrNi3MoV steel with high hardness, hardened by conventional technology, also had reduced wear resistance.

**Author Contributions:** Conceptualization, S.B. and E.P.; methodology, O.B.; validation, P.K., T.G. and O.B.; formal analysis, T.G.; investigation, O.B.; data curation, S.B.; writing—original draft preparation, S.B.; writing—review and editing, E.P. and P.K.; visualization, T.G.; supervision, P.K. All authors have read and agreed to the published version of the manuscript.

**Funding:** This research received no external funding.

**Institutional Review Board Statement:** Not applicable.

**Informed Consent Statement:** Not applicable.

**Data Availability Statement:** The data are unavailable due to privacy restrictions.

**Conflicts of Interest:** The authors declare no conflict of interest.

## References

1. Shneiderman, A.S. Transformations during high tempering in steel 25KhN3MFA. *Met. Sci. Heat Treat.* **1980**, *22*, 862–864. [[CrossRef](#)]
2. Leshchenko, A.N.; Vishnyakov, A.P. Investigation of the kinetics of the transformation of austenite in chromium-nickel steel 38KhN3MFA. *Metall. Gornorudn. Promyshlennost* **2000**, *1*, 49–50. (In Russian)
3. Golubev, A.E.; Sergeev, Y.G. Isothermal hardening of steel 38KhN3MFA. In Proceedings of the International Scientific Conference XXX Yubileynaya Nedelya Nauki SPb GTU, Sankt-Peterburg, Russia, 26 November–1 December 2002; Volume VI, pp. 38–39. (In Russian)
4. Kuznetsova, D.P. Influence of temperature-time parameters of tempering on the hardness of 38KhN3MFA steel hardened to martensite. In Proceedings of the II Mezhdunarodnaya Nauchnaya Shkola Dlya Molodezhi «Materialovedenie i Metallofizika Legkih Splavov», Ekaterinburg, Russia, 12–16 November 2012; pp. 104–106. (In Russian)
5. Bobyr, S.V.; Krot, P.V.; Levchenko, G.V.; Baranovska, O.E.; Loschkarev, D.V. Influence of modes of thermal hardening and the subsequent cryogenic processing on structure and properties of steel 38Ni3CrMoV. *Metalozn. Obrobka Met.* **2021**, *27*, 14–22. [[CrossRef](#)]
6. Önem, O.U. Effect of Temperature on Fatigue Properties of DIN 35NiCrMoV12.5 Steel. Master's Thesis, Middle East Technical University, Ankara, Turkey, 2003.
7. Aksu, E. The Effect of Austempering Parameters on Impact and Fracture Toughness of DIN 35NiCrMoV12.5 Gun Barrel Steel. Master's Thesis, Middle East Technical University, Ankara, Turkey, 2005.
8. Baldissera, P.; Delprete, C. Deep cryogenic treatment: A bibliographic review. *Open Mech. Eng. J.* **2008**, *2*, 1–11. [[CrossRef](#)]
9. Senthilkumar, D. Cryogenic treatment: Shallow and deep. In *Encyclopedia of Iron, Steel, and Their Alloys*; Totten, G.E., Colas, R., Eds.; Taylor and Francis: New York, NY, USA, 2016; pp. 995–1007. [[CrossRef](#)]
10. Prudhvi, K.; Lakshmi, V.V. Cryogenic Tool Treatment. *Imp. J. Interdiscip. Res.* **2016**, *2*, 1204–1211. [[CrossRef](#)]
11. Jovicevic-Klug, M.; Jovicevic-Klug, P.; Kranjec, T.; Podgornik, B. Cross-effect of surface finishing and deep cryogenic treatment on corrosion resistance of AISI M35 steel. *J. Mater. Res. Technol.* **2021**, *14*, 2365–2381. [[CrossRef](#)]
12. Jurci, P.; Domankova, M.; Ptacinova, J.; Pasak, M.; Kusy, M.; Priknerova, P. Investigation of the Microstructural Changes and Hardness Variations of Sub-Zero Treated Cr-V Ledeburitic Tool Steel Due to the Tempering Treatment. *J. Mater. Eng. Perform.* **2018**, *27*, 1514–1529. [[CrossRef](#)]
13. Jovicevic-Klug, P.; Kranjec, T.; Jovicevic-Klug, M.; Kosec, T.; Podgornik, B. Influence of the deep cryogenic treatment on AISI 52100 and AISI D3 steel's corrosion resistance. *Materials* **2021**, *14*, 6357. [[CrossRef](#)]
14. Collins, D.N.; Dormer, J. Deep cryogenic treatment of a D2 cold-work tool steel. *Heat Treat. Met.* **1997**, *3*, 71–74.
15. Krot, P.; Bobyr, S.; Zharkov, I.; Prykhodko, I.; Borkowski, P. Increasing the durability of critical parts in heavy-duty industrial machines by deep cryogenic treatment. In *Fatigue and Fracture of Materials and Structures*; Lesiuk, G., Duda, S., Correia, J.A.F.O., De Jesus, A.M.P., Eds.; Springer: Cham, Switzerland, 2022; Volume 24, pp. 127–133. [[CrossRef](#)]
16. Kalia, S. Cryogenic processing: A study of materials at low temperatures. *J. Low Temp. Phys.* **2010**, *158*, 934–945. [[CrossRef](#)]
17. Villa, M.; Somers, M.A.J. Cryogenic treatment of steel: From concept to metallurgical understanding. In Proceedings of the 24th International Federation for Heat Treatment and Surface Engineering Congress (IFHTSE 2017), Nice, France, 26–29 June 2017.
18. Collins, D.N. Deep cryogenic treatment of tool steels: A review. *Heat Treat. Met.* **2010**, *23*, 40–42. [[CrossRef](#)]
19. Krot, P.; Bobyr, S.; Dedik, M. Simulation of backup rolls quenching with experimental study of deep cryogenic treatment. *Int. J. Microstruct. Mater. Prop.* **2017**, *12*, 259–275. [[CrossRef](#)]
20. Jovicevic-Klug, P.; Podgornik, B. Review on the effect of deep cryogenic treatment of metallic materials in automotive applications. *Metals* **2020**, *10*, 434. [[CrossRef](#)]
21. Chinnasamy, M.; Rathanasamy, R.; Palaniappan, S.K.; Pal, S.K. Microstructural transformation analysis of cryogenic treated conical rock cutting bits for mining applications. *Int. J. Ref. Met. Hard Mater.* **2023**, *110*, 105995. [[CrossRef](#)]
22. Cardoso, P.H.S.; Israel, C.L.; da Silva, M.B.; Klein, G.A.; Soccol, L. Effects of deep cryogenic treatment on microstructure, impact toughness and wear resistance of an AISI D6 tool steel. *Wear* **2020**, *456–457*, 203382. [[CrossRef](#)]
23. Gobbi, S.J.; Gobbi, V.J.; Reinke, G. Ultra Low Temperature process effects on micro-scale abrasion of tool steel AISI D2. *Mater. Sci. Technol.* **2018**, *35*, 1355–1364. [[CrossRef](#)]

24. Korade, D.; Ramana, K.V.; Jagtap, K. Wear and Fatigue Behaviour of Deep Cryogenically Treated H21 Tool Steel. *Trans. Indian Inst. Met.* **2020**, *73*, 843–851. [[CrossRef](#)]
25. Voglar, J.; Novak, Ž.; Jovičević-Klug, P.; Podgornik, B.; Kosec, T. Effect of deep cryogenic treatment on corrosion properties of various high-speed steels. *Metals* **2021**, *11*, 14. [[CrossRef](#)]
26. Razavykia, A.; Delprete, C.; Baldissera, P. Correlation between microstructural alteration, mechanical properties and manufacturability after cryogenic treatment: A review. *Materials* **2019**, *12*, 3302. [[CrossRef](#)]
27. Jimbert, P.; Iturrondobeitia, M.; Ibarretxe, J.; Fernandez-Martinez, R. Influence of cryogenic treatment on wear resistance and microstructure of AISI A8 tool steel. *Metals* **2018**, *8*, 1038. [[CrossRef](#)]
28. Ciski, A.; Nawrocki, P.; Babul, T.; Hradil, D. Multistage cryogenic treatment of X153CrMoV12 cold work steel. *IOP Conf. Ser. Mater. Sci. Eng.* **2018**, *461*, 012012. [[CrossRef](#)]
29. Zhou, G.; Deng, S.; Wei, W.; Liu, Q. Effect of multiple deep cryo-treating and tempering on microstructure and property evolution of high carbon bearing steel. *Mater. Res. Express* **2020**, *7*, 066529. [[CrossRef](#)]
30. Jurči, P.; Ptačinová, J.; Sahul, M.; Dománková, M.; Dlouhy, I. Metallurgical principles of microstructure formation in sub-zero treated cold-work tool steels—A review. *Matériaux Tech.* **2018**, *106*, 104–113. [[CrossRef](#)]
31. Ray, K.K.; Das, D. Improved wear resistance of steels by cryotreatment: The current state of understanding. *Mater. Sci. Technol.* **2016**, *33*, 340–354. [[CrossRef](#)]
32. Li, B.; Li, C.; Wang, Y.; Jin, X. Effect of cryogenic treatment on microstructure and wear resistance of carburized 20CrNi2MoV steel. *Metals* **2018**, *8*, 808. [[CrossRef](#)]
33. Wang, K.; Gu, K.; Misra, R.D.K.; Chen, L.; Liu, X.; Weng, Z.; Wang, J. On the optimization of microstructure and mechanical properties of CrWMn tool steel by deep cryogenic treatment. *Steel Res. Int.* **2019**, *90*, 1800523. [[CrossRef](#)]
34. Antony, A.; Schmer, N.; Sokolova, A.; Mahjoub, R.; Fabijanic, D.; Stanford, N. Quantification of the dislocation density, size, and volume fraction of precipitates in deep cryogenically treated martensitic steels. *Metals* **2020**, *10*, 1561. [[CrossRef](#)]
35. Gavriljuk, V.G.; Theisen, W.; Sirosh, V.V.; Polshin, E.V.; Kortmann, A.; Mogilny, G.S.; Petrov, Y.N.; Tarusin, Y.V. Low-temperature martensitic transformation in tool steels in relation to their deep cryogenic treatment. *Acta Mater.* **2013**, *61*, 1705–1715. [[CrossRef](#)]
36. Jovicevic-Klug, P.; Jovicevic-Klug, M.; Sever, T.; Feizpour, D.; Podgornik, B. Impact of steel type, composition and heat treatment parameters on effectiveness of deep cryogenic treatment. *J. Mater. Res. Technol.* **2021**, *14*, 1007–1020. [[CrossRef](#)]
37. Villa, M.; Somers, M.A.J. Cryogenic treatment of an AISI D2 steel: The role of isothermal martensite formation and “martensite conditioning”. *Cryogenics* **2020**, *110*, 103131. [[CrossRef](#)]
38. Jovicevic-Klug, P.; Jenko, M.; Jovicevic-Klug, M.; Setina Batic, B.; Kovac, J.; Podgornik, B. Effect of deep cryogenic treatment on surface chemistry and microstructure of selected high-speed steels. *Appl. Surf. Sci.* **2021**, *548*, 149257. [[CrossRef](#)]
39. Huang, J.Y.; Zhu, Y.T.; Liao, X.Z.; Beyerlein, I.J.; Bourke, M.A.; Mitchell, T.E. Microstructure of cryogenic treated M2 tool steel. *Mater. Sci. Eng. A* **2003**, *339*, 241–244. [[CrossRef](#)]
40. Zare, A.; Mansouri, H.; Hosseini, S.R. Influence of the holding time of the deep cryogenic treatment on the strain hardening behavior of HY-TUF steel. *Int. J. Mech. Mater. Eng.* **2015**, *10*, 306. [[CrossRef](#)]
41. Yuan, X.H.; Yang, M.S.; Zhao, K.Y. Effects of microstructure transformation on strengthening and toughening for heat-treated low carbon martensite stainless bearing steel. *Mater. Sci. Forum* **2015**, *817*, 667–674. [[CrossRef](#)]
42. Xie, C.; Zhou, L.; Min, N.; Wu, X. Effect of deep cryogenic treatment on carbon segregation in Cr8Mo2SiV tool steel during tempering. *Philos. Mag. Lett.* **2017**, *97*, 372–377. [[CrossRef](#)]
43. Weng, Z.; Gu, K.; Wang, K.; Liu, X.; Wang, J. The reinforcement role of deep cryogenic treatment on the strength and toughness of alloy structural steel. *Mater. Sci. Eng. A* **2020**, *772*, 138698. [[CrossRef](#)]
44. Li, S.; Wu, X. Microstructural evolution and corresponding property changes after deep cryotreatment of tool steel. *Mater. Sci. Technol.* **2015**, *31*, 1867–1878. [[CrossRef](#)]
45. Sonar, T.; Lomte, S.; Gogte, C. Cryogenic Treatment of Metal—A Review. *Mater. Today Proc.* **2018**, *5*, 25219–25228. [[CrossRef](#)]
46. Gill, S.S.; Singh, J.; Singh, R.; Singh, H. Metallurgical principles of cryogenically treated tool steels—A review on the current state of science. *Int. J. Adv. Manuf. Technol.* **2010**, *54*, 59–82. [[CrossRef](#)]
47. Li, S.; Min, N.; Li, J.; Wu, X.; Li, C.; Tang, L. Experimental verification of segregation of carbon and precipitation of carbides due to deep cryogenic treatment for tool steel by internal friction method. *Mater. Sci. Eng. A* **2013**, *575*, 51–60. [[CrossRef](#)]
48. Li, S.; Xiao, M.; Ye, G.; Zhao, K.; Yang, M. Effects of deep cryogenic treatment on microstructural evolution and alloy phases precipitation of a new low carbon martensitic stainless bearing steel during aging. *Mater. Sci. Eng. A* **2018**, *732*, 167–177. [[CrossRef](#)]
49. Tyshchenko, A.; Theisen, W.; Oppenkowski, A.; Siebert, S.; Razumov, O.; Skoblik, A.; Sirosh, V.; Petrov, Y.; Gavriljuk, V. Low-temperature martensitic transformation and deep cryogenic treatment of a tool steel. *Mater. Sci. Eng. A* **2010**, *527*, 7027–7039. [[CrossRef](#)]
50. Gavriljuk, V.G.; Firstov, S.A.; Sirosh, V.A.; Tyshchenko, A.I.; Mogilny, G.S. Carbon distribution in low temperature isothermal iron based martensite and its tetragonality. *Metallofiz. Noveishie Teknol.* **2016**, *38*, 455–475. [[CrossRef](#)]
51. Preciado, M.; Pellizzari, M. Influence of deep cryogenic treatment on the thermal decomposition of Fe–C martensite. *J. Mater. Sci.* **2014**, *49*, 8183–8191. [[CrossRef](#)]
52. Kumar, T.V.; Thirumurugan, R.; Viswanath, B. Influence of cryogenic treatment on the metallurgy of ferrous alloys: A review. *Mater. Manuf. Process.* **2017**, *32*, 1789–1805. [[CrossRef](#)]

53. Lee, S.-J.; Lusk, M.; Lee, Y.-K. Conversional model of transformation strain to phase fraction in low alloy steels. *Acta Mater.* **2007**, *55*, 875–882. [[CrossRef](#)]
54. Inoue, T.; Raniecki, B. Determination of thermal-hardening stress in steels by use of thermoplasticity theory. *J. Mech. Phys. Solids* **1978**, *26*, 187–212. [[CrossRef](#)]
55. Danilchenko, V.; Filatov, A.; Mazanko, V.F.; Iakovlev, V.E. Cyclic martensitic transformations influence on the diffusion of carbon atoms in Fe-18 wt.%Mn-2 wt.%Si alloy. *Nanoscale Res. Lett.* **2017**, *12*, 194. [[CrossRef](#)]
56. Morsdorf, L.; Tasan, C.; Ponge, D.; Raabe, D. 3D structural and atomic-scale analysis of lath martensite: Effect of the transformation sequence. *Acta Mater.* **2015**, *95*, 366–377. [[CrossRef](#)]
57. Bobyr, S.V.; Parusov, E.V.; Levchenko, G.V.; Borisenko, A.Y.; Chuiko, I.M. Shear transformation of austenite in steels considering stresses effects. *Prog. Phys. Met.* **2022**, *23*, 379–410. [[CrossRef](#)]

**Disclaimer/Publisher’s Note:** The statements, opinions and data contained in all publications are solely those of the individual author(s) and contributor(s) and not of MDPI and/or the editor(s). MDPI and/or the editor(s) disclaim responsibility for any injury to people or property resulting from any ideas, methods, instructions or products referred to in the content.